

Inhibition formalisms of Sb catalytic in BHET-glycol systems

Pedro de Oliveira Abi Rached¹, Prof. Dr. Maria do Rosário Gomes Ribeiro¹, Dr. Adrien Mekki-Berrada²

¹ Department of Chemical Engineering, Instituto Superior Técnico, Lisbon, Portugal.

² Institut Français du Pétrole – Énergies nouvelles (IFPEN), Solaize, France.

Abstract

The synthesis of PET involves the polycondensation of bis(2-hydroxyethyl) terephthalate (BHET). This reaction is catalysed by species containing antimony (Sb), such as antimony (III) oxide (Sb_2O_3). Besides being a product of the reaction, ethylene glycol (EG) is also added to the system in order to dissolve Sb_2O_3 and form what is believed to be the catalytically active species, antimony (III) glycolate ($\text{Sb}(\text{Gly})_2$). However, EG is also believed to inhibit the catalytic activity of Sb_2O_3 by further reacting with $\text{Sb}(\text{Gly})_2$ to form antimony (V) glycolate ($\text{Sb}(\text{Gly})_3$).

The objective of this work was to perform a kinetic study of a synthetic PET (re)polymerisation system involving purified BHET and EG as starting materials, and Sb_2O_3 as catalyst. The reaction was performed at different ranges of Sb concentration, $[\text{Sb}]$, initial ratio of BHET and EG fed to the reactor, $\text{BHET}_0:\text{EG}_0$, and temperature (170, 180 and 190°C), and using different precursors of Sb_2O_3 (powder and dissolved). The rate of reaction was observed to be directly proportional to the temperature and $[\text{Sb}]$, but no clear conclusions about the inhibitory effect of EG could be drawn.

For this reason, in order to ascertain whether EG presents an inhibitory effect on the catalytic activity of Sb_2O_3 , a modelling work was carried out in order to tune parameters of existing reactor models and to propose a new reactor model capable of predicting accurately the experimental results for all ranges of experimental conditions. The simplest model, which did not account for the inhibition of Sb_2O_3 by EG, was able to predict well the experimental results when EG_0 was below 25 wt-%, while the more sophisticated models, which took the inhibition into account, were also able to also predict well the behaviour of the system when EG_0 was equal or greater than 25 wt-%.

Keywords: PET, antimony, ethylene glycol, kinetic study, catalysis, catalytic inhibition, modelling.

1 Introduction

1.1 PET production, uses and recycling

Poly(ethylene terephthalate), more commonly known as PET, is a thermoplastic polyester with excellent chemical and physical properties for many uses, which include bottling and packaging, fibres for clothing and automotive parts [1].

In 2016, 485 billion PET bottles were produced. This number is expected to increase to 583 billion in 2021 [2]. Plastic products' main application are short-term living and disposable packaging material, which become waste after single-use. From 1950 to 2015, it is estimated that 6.3 billion tons of plastic waste was generated, around which 9% was recycled, 12% was incinerated and 79% was accumulated in landfills or in nature [3].

Hence, a big amount of plastic waste has been accumulated in the environment and, each year,

around one million metric tons of plastic end up in landfill or in the ocean [3].

Recycling is the best method for PET waste management, as it provides opportunities for reducing the dependency on fossil fuels as a raw material in PET production (thus minimizing carbon dioxide (CO_2) emissions) and decrease the load on landfill space [4]. Thus, recycled PET (rPET) has a prospective to substitute virgin PET from refined fossil fuels.

Mechanical recycling allows for the closed-loop recycling of transparent PET, to give products which are fitted for the original application [5]. However, mechanical recycling only allows for the open-loop recycling of coloured PET, to give products which are not fitted for the original applications [5]. For this reason, chemical recycling is studied as an alternative to achieve closed-loop recycling of PET for all types of PET [5]. Amongst the possible routes of chemical recycling,

glycolysis is one of the most promising, due to its mild conditions and weak volatility of EG [6]. The product of glycolysis is BHET, which can be purified and (re)polymerised to rPET.

Sb-based catalysts, such as antimony (III) oxide (Sb_2O_3) and antimony (III) acetate ($\text{Sb}(\text{Ac})_3$), are the most widely used catalysts in industry for the polycondensation of BHET to PET [1]. These compounds remain trapped in the PET throughout its life in small concentrations ($220 < [\text{Sb}] < 240$ ppm), and can therefore be reused as catalysts in the glycolysis of PET at the end of its life [7]. These are called inherited catalysts.

The objective of the current work was to perform the kinetic study of a synthetic PET (re)polymerisation system comprising BHET (obtained from the glycolysis of PET) and EG as starting materials, and Sb_2O_3 as catalyst. The BHET had been previously purified, as to not contain inherited catalyst metals and dyes, and guarantee that all Sb_2O_3 came from external addition, thus allowing for an accurate quantification of the amount of catalyst present in the system.

Sb_2O_3 is believed to be a homogeneous catalyst in the polymerisation of PET and it must first react with EG to produce antimony (III) glycolate, $\text{Sb}(\text{Gly})_2$, which is believed to be the catalytically active form of Sb [8]. This reaction is shown in Figure 1.

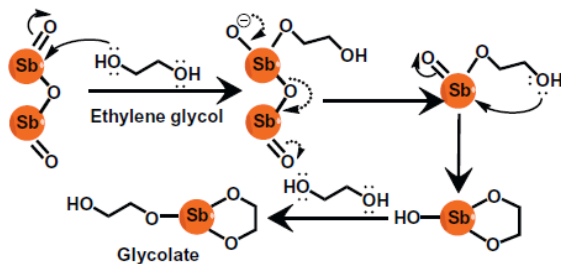


Figure 1: Activation of Sb_2O_3 by EG to form $\text{Sb}(\text{Gly})_2$.

Although EG is necessary to activate Sb_2O_3 , it has also been shown that Sb_2O_3 is not catalytically active in OH-rich media, due to the formation of stable Sb-glycolate complexes [9]. Given that EG contains OH groups, it has been proposed that EG could further react with $\text{Sb}(\text{Gly})_2$ to give antimony (V) glycolate, $\text{Sb}(\text{Gly})_3$, whose ionic form, shown in Figure 2, is highly stable and isolatable [9], [10]. This means that Sb remains trapped as $\text{Sb}(\text{Gly})_3$, thus decreasing the amount of Sb available to catalyse the polymerisation of PET. For this reason, EG is said to also inhibit the catalytic activity of Sb_2O_3 , and this phenomenon is especially significant at high [EG].

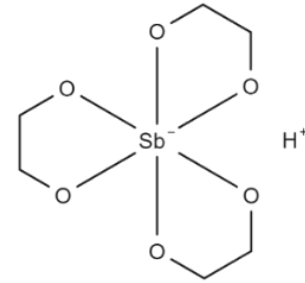


Figure 2: Ionic form of $\text{Sb}(\text{Gly})_3$.

The experimental kinetic study and the modelling of the reactor system aimed to verify the presence of the inhibitory effect of EG and the ranges of reaction compositions in which it was most visible.

1.2 Reaction kinetics

As will be explained later, the polymerisation of PET is a step-growth process, consisting of a series of reversible reactions, whose general equation is shown in Equation (1), where PET_m and PET_n refer to oligomers of PET which react to produce the longer oligomer PET_{m+n} and EG.



In the present work, the process was carried out in a single batch reactor and at temperatures below the boiling point of EG, meaning that there was no way to remove the EG produced. For this reason, only the reactions producing oligomers up to PET_4 were considered and the formation of longer-chain oligomers was considered negligible. The reactions are shown in Table 1.

Table 1: Reactions considered.

R₁	$2 \times \text{BHET} \xrightleftharpoons{k_{1 \rightarrow}} \text{PET}_2 + \text{EG}$
R₂	$\text{BHET} + \text{PET}_2 \xrightleftharpoons{k_{2 \rightarrow}} \text{PET}_3 + \text{EG}$
R₃	$\text{BHET} + \text{PET}_3 \xrightleftharpoons{k_{3 \rightarrow}} \text{PET}_4 + \text{EG}$
R₄	$2 \times \text{PET}_2 \xrightleftharpoons{k_{4 \rightarrow}} \text{PET}_4 + \text{EG}$

The general formula of the rate equation for a reversible reaction is shown in Equation (2), where $k_{j \rightarrow}$ and $K_{\text{eq}j}$ refer to the forward rate constant and the equilibrium constant, respectively, for each reaction j , Q_q and P_p refer to the reactants and products, respectively, involved in each reaction j , $\nu_{p,j}$ and $\nu_{q,j}$ and refer to the stoichiometric coefficients of each reactant and product, respectively, involved in each reaction j .

$$r_j = k_{j \rightarrow} \times \left(\prod_{p \in j} [P_p]^{\nu_{p,j}} - \frac{\prod_{q \in j} [Q_q]^{\nu_{q,j}}}{K_{\text{eq}j}} \right) \quad (2)$$

2 Experimental part

2.1 Materials

EG (99.5%) was supplied by Carlo Erba, Sb_2O_3 (99%) was supplied by Sigma-Aldrich, and BHET obtained from the glycolysis of PET.

2.2 Methodology

As a good temperature control is desired for the present work, a dry bath heater was chosen in order to accommodate the reactors and bring them to the desired temperatures for the reaction. In order to reduce heat losses and better control the temperature, a heating blanket was wrapped around the dry bath and some wool was also put around the reactors to cover them.

Two types of reactors were used: autoclaves and glass reactors. The choice of reactor was done based on the type of process to be carried out, as will be explained forward. The reactors had magnetic agitation and there were two type S thermocouples available for temperature measurement.

2.2.1 Preparation of the mother solution

Sb_2O_3 is a fine white powder. This can be added directly to the reactor, in which case it must dissolve in the reaction medium in order to function as a catalyst. For this reason, Sb_2O_3 powder is a heterogeneous precursor.

On the other hand, Sb_2O_3 can be previously dissolved in EG to make a mother solution, which is then added to the reactor. This mother solution works as a homogeneous precursor of Sb_2O_3 .

A mother solution of 1 wt-% of Sb_2O_3 in EG (MS1%) was envisaged, which is equivalent to [Sb] of 8353 ppm. Two solutions of about 100 g (100 mL) each were prepared.

Additionally, to facilitate dissolution, the process was to be carried out at 200°C and 1500 rpm. The boiling point of EG at atmospheric pressure is 197°C, so it was expected that, despite strong agitation, some of the EG would evaporate, which would lead to a build-up of pressure inside the closed reactor.

For this reason, an autoclave reactor, which is capable of withstanding high pressures (<0.4 GPa) and temperatures (<600°C) for long periods of time, was used. The masses of EG and Sb_2O_3 added to each autoclave in order to prepare the solutions are shown in Table 2.

Table 2: Masses of EG and Sb_2O_3 and resulting [Sb] in each autoclave.

Autoclave	Mass EG (g)	Mass Sb_2O_3 (g)	[Sb] (ppm)
1	100.13	1.03	8.50×10^3
2	99.98	1.00	8.27×10^3

2.2.2 Operating conditions

The main variables whose effect on the reaction rate was desired to be studied were [Sb], $\text{BHET}_0:\text{EG}_0$, temperature and the precursor of Sb_2O_3 (MS1% or Sb_2O_3 powder).

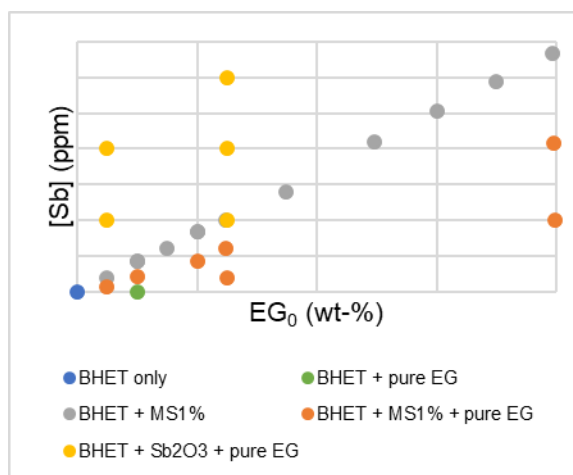


Figure 3: Map of compositions, where $\text{EG}_0 = 1 - \text{BHET}_0$.

Figure 3 shows that the use of Sb_2O_3 powder allowed for the preparation of compositions not possible had MS1% been used, *i.e.*, high [Sb] and low EG_0 .

2.2.3 Experimental procedure

2.2.3.1 Loading reactors

As shown in Figure 3, due to the big number of compositions to study, it was necessary to have as many reactors as possible working at a given time. For this reason, the reactions were carried out in glass reactors, instead of autoclaves.

Glass reactors, despite being more practical and easier to use, are more fragile and prone to breakage if there is a build-up of pressure inside it. For this reason, the reference temperature, T_{ref} , was chosen as 180°C. This choice allowed for the performance of the reaction at lower and higher temperatures (170 and 190°C) while still being below the boiling point of EG and maintaining a high rate of reaction.

After calculating the necessary mass of each reagent to be added to the reactor to make up a total mass of 10 g, the desired mass of BHET was

added to the reactor with a spatula. Then, the required masses of MS1% and pure EG were added using Pasteur pipettes, and the required mass of Sb_2O_3 powder was transferred with the aid of a weighing boat.

2.2.3.2 Reaction times

After filling up the reactors, they were put in the dry bath heater and the two thermocouples available for the temperature measurement were placed inside two reactors. The dry bath heater was then turned on to start the heating and bring the reactors up to the target temperature, T_{target} .

Once T_{target} was reached, the stopwatch was started. Due to the high temperature of the reactors, it would be difficult to take samples, because it would involve opening the lid of each reactor at a given time and taking samples (e.g., with a glass pipette), which would need to be quickly transferred to another recipient, otherwise they would solidify. Furthermore, when opening the lid, there could be evaporation of the reaction medium and a temperature drop.

For these reasons, sampling of the reactors was not done. Instead of preparing six reactors with six different compositions, every two reactors were prepared with the same composition, giving three pairs of reactors with three different compositions in the dry bath heater at a given run. Each reactor in the pair was removed and had the reaction stopped at a different time, in order to be analysed and obtain information about the composition and, subsequently, the rate of reaction.

By following this procedure, it would be possible to obtain information about the progress of the reaction at three different times: t_0 (initial composition), t_1 (when one of the reactors in the pair was removed) and t_2 (when the second reactor in the pair was removed). The choice of t_1 and t_2 was done individually for each pair of compositions. In general, the lower [Sb] and the higher EG_0 , the lower the rate of reaction is expected to be and, for this reason, the bigger the values of t_1 and t_2 chosen.

2.2.3.3 Sampling

The reactions were stopped by placing the glass reactors inside a cold-water bath, in order to quickly decrease its temperature and solidify the contents inside it. The solidified product was then broken with the help of a metal spatula and transferred to a small glass flask to be sent to analysis.

2.2.4 Analytical techniques

Size-exclusion chromatography (SEC) and high-performance liquid chromatography (HPLC) were the analytical techniques used in the current work.

All samples were analysed by SEC, which had two types of detectors: a refractive index (RI) and an ultraviolet detector (UV). The former is less sensitive, but can identify any type of component in the analyte, while the latter requires that the compound interact with UV radiation to be detectable, thus not allowing for the detection of alcoholic species (e.g., EG and DEG) [11].

For this reason, the effluent was first passed through the RI detector, in order to be able to tell apart the terephthalic species from EG and DEG (glycols). It was then passed through the UV detector in order to uniquely quantify the terephthalic species.

Not all samples were passed through HPLC, due to a longer analysis time, and it only employed an UV detector, thus unable to quantify EG. Thus, the HPLC results were only used for comparison with SEC, to see if they followed a similar behaviour and trend. The relative uncertainty in both analytical techniques was estimated to be $\pm 10\%$.

3 Experimental results

3.1 Effect of [Sb]

The experiments were made at constant $\text{BHET}_0:\text{EG}_0$ and only the catalyst concentration was varying. Figure 4 shows three different experiments, with [Sb] equal to 0, A and B ppm, where $A < B$.

As [Sb] increases, the rate of reaction also increases, given the higher conversion of BHET in a given period of time. It is also possible to observe a clear difference between the results when [Sb] = 0 ppm, *i.e.*, the reaction is uncatalysed, and the results when the reaction is catalysed. As shown in Figure 4, the uncatalysed reaction proceeds much more slowly than the catalysed reaction, even at small [Sb], which highlights the importance of the use of catalyst in the industrial polymerisation of PET, in order to have a faster and more energy-efficient process.

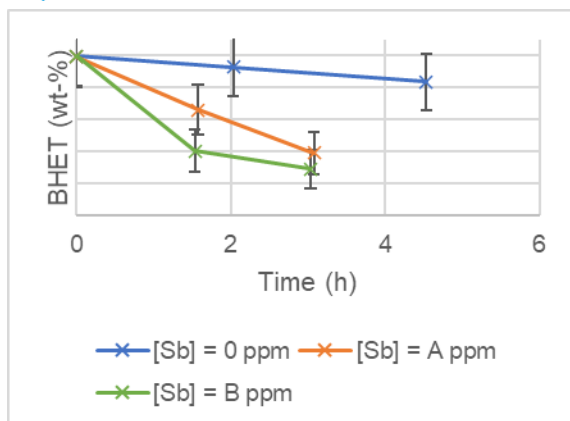


Figure 4: BHET VS time for $T=180^{\circ}\text{C}$ and varying $[\text{Sb}]$.

3.2 Effect of $\text{BHET}_0:\text{EG}_0$

The rate of an equilibrium reaction is affected by the initial concentration of reactants and the driving force for the reaction. In the case of the studied system, the only reactant was BHET, and it was expected that a greater initial concentration of BHET, given by a higher $\text{BHET}_0:\text{EG}_0$, would mean that there would be initially a higher number of molecules available to react, thus giving a higher initial rate of reaction.

At the same time, the driving force for the reaction is given by the magnitude of $\Delta_r G$, which is translated by a bigger difference between K and K_{eq} , *i.e.*, when $\text{BHET}_0:\text{EG}_0$ is further away from the equilibrium composition, $\text{BHET}_{\text{eq}}:\text{EG}_{\text{eq}}$. It was observed that $\text{BHET}_{\text{eq}}:\text{EG}_{\text{eq}}$ was inferior to all of the $\text{BHET}_0:\text{EG}_0$ attempted, which means that, as BHET_0 increases, both the probability of successful collisions between reactant molecules and the magnitude of $\Delta_r G$ increase, so that the rate of reaction is also expected to increase.

Additionally, $\text{BHET}_0:\text{EG}_0$ will also affect the inhibition effect of EG on Sb because, the greater EG_0 , translated by a smaller $\text{BHET}_0:\text{EG}_0$, the greater the inhibition effect is expected to be, which also means a smaller rate of reaction.

All of these factors lead to the expectation that, as $\text{BHET}_0:\text{EG}_0$ increases, the rate of reaction will also increase. However, this is not always observed. Figure 5 shows three different tests performed at high contents of $[\text{Sb}]$, 180°C and using MS1%, but at varying $\text{BHET}_0:\text{EG}_0$. When EG_0 increased, the effect on the rate of reaction was not evident. However, it is clear that the rate of reaction was significantly smaller when EG_0 was high. This result is expected, given the low value of BHET_0 (lower probability of collision between

reactant molecules and smaller driving force), and also given the high EG_0 (great inhibition of the catalytic activity of Sb).

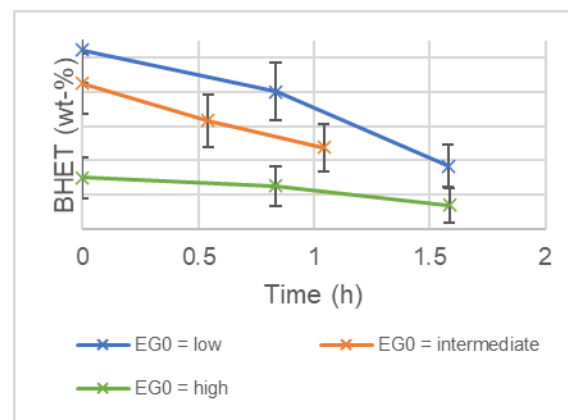


Figure 5: BHET VS time for $T=180^{\circ}\text{C}$ and varying EG_0 .

3.3 Effect of temperature

From Figure 6, it is clearly visible that an increase in temperature leads to an increase in the rate of reaction. A higher temperature means that a higher number of molecules will have enough energy to give successful collisions, which lead to a reaction, which translates in a greater rate of reaction.

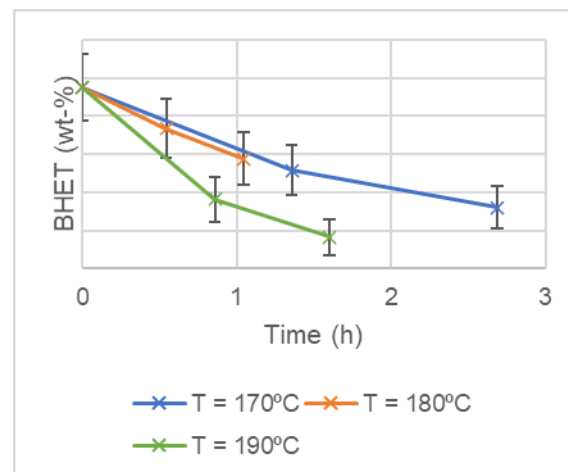


Figure 6: BHET VS time for varying temperature.

3.4 Effect of the precursor of catalyst

As mentioned previously, given that the reaction happens in liquid phase, MS1% is the homogeneous precursor and Sb_2O_3 powder is the heterogeneous precursor, which must be dissolved in order to become catalytically active.

The rate of dissolution of a solid is directly proportional to the temperature, agitation and surface area. The preparation of MS1% employed the

same Sb_2O_3 powder and proceeded at higher temperature (200°C) and agitation (1500 rpm). Despite that, it still took several hours to completely dissolve the powder. For this reason, it is expected that the rate of reaction be greater when using MS1% as opposed to Sb_2O_3 powder as the precursor of catalyst.

Figure 7 shows six sets of results with increasing [Sb]. It is clear that an increase in [Sb] causes an increase in the rate of reaction both in the case of MS1% and Sb_2O_3 powder. Only for [Sb] = 5X ppm was the reaction performed using both MS1% and Sb_2O_3 powder. Despite the initial belief, the reaction appeared to proceed faster when using the powder. Possible explanations are the uncertainty in the mass of Sb_2O_3 powder added to the reactor, due to the very small amounts used, and the thin nature of the powder.

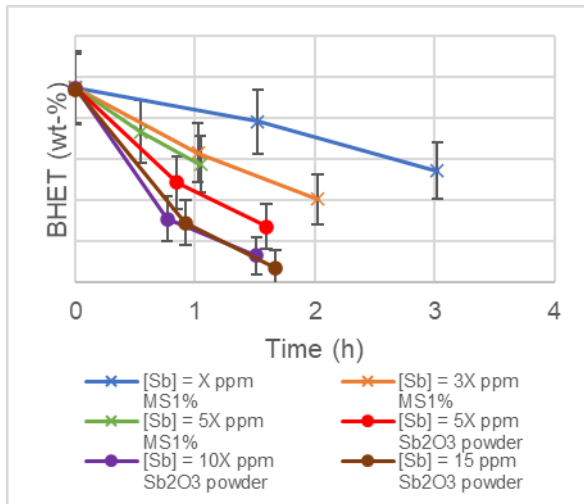


Figure 7: BHET VS time for $T=180^\circ\text{C}$, varying [Sb] and catalyst precursors.

However, it is possible to see from Figure 7 that there is no apparent change in the reaction rate when [Sb] increases from 10X ppm to 15X ppm. This could mean that Sb_2O_3 has reached its limit of solubility in EG at 180°C or that it did not have enough time for dissolve and become catalytically active, as the reaction was allowed to proceed for less than 2 h. This would cause the real value of [Sb] to be smaller than that if all Sb_2O_3 had dissolved. If this limit of solubility was between 5X ppm and 10X ppm, then the rates of reaction in both cases should be the approximately equal.

4 Modelling

4.1 Equilibrium constants

In order to make the reactor model, it was necessary to define Equation (2) for all four reactions

shown in Table 1. As reactions were not carried until equilibrium in the current work, the values of K_{eq} were obtained from previous work performed at IFPEN on a similar system. These values are shown in Table 3.

Table 3: Final values of K_{eq} for each reaction.

K_{eq_1}	K_{eq_2}	K_{eq_3}	K_{eq_4}
0.9	1.6	1	1

4.2 Activity formalism

It is possible to split $k_{j\rightarrow}$ into a noncatalytic (thermal) term, $k_{j\rightarrow}^{\text{th}}$, and a catalytic term, $k_{j\rightarrow}^{\text{cat}}$ [12]. Both terms are dependent on the temperature of the system, but the latter may also be dependent on several other factors, such as [Sb], [EG] and other parameters, e.g., α_1 and α_2 , depending on how it is defined.

By defining a formalism for the catalytic activity of Sb, \mathcal{FM} , which may take into account both its catalytic activity and the inhibition effects on it, it is possible to decorrelate the dependency of $k_{j\rightarrow}^{\text{cat}}$ on [Sb], [EG] and other parameters, and leave it only dependent on the temperature. The resulting expression is shown in Equation (3).

$$k_{j\rightarrow}(T) = k_{j\rightarrow}^{\text{th}}(T) + k_{j\rightarrow}^{\text{cat}}(T) \times \mathcal{FM}([\text{Sb}], [\text{EG}], \alpha_1, \alpha_2, \dots) \quad (3)$$

Fitting one different $k_{j\rightarrow}$ for each reaction j , all with their individual $k_{j\rightarrow}^{\text{th}}$, $k_{j\rightarrow}^{\text{cat}}$ and other parameters, would cause great correlation and interdependency between these parameters, which would render their estimation difficult, due to the limited sensitivity of the experimental database. For this reason, only one $k_{j\rightarrow}$ for all four reactions was considered, with only one set of parameters to fit. The resulting expression is shown in Equation (4), with the parameters to fit shown in bold. The remaining step would be to substitute \mathcal{FM} by existing activity formalisms.

$$k(T) = \{ \mathbf{k}_{\text{ref}}^{\text{th}} + \mathbf{k}_{\text{ref}}^{\text{cat}} \times \mathcal{FM}([\text{Sb}], [\text{EG}], \alpha_1, \alpha_2, \dots) \} \times \exp\left(-\frac{E_a}{R} \left[\frac{1}{T} - \frac{1}{T_{\text{ref}}} \right]\right) \quad (4)$$

4.3 Formalisms from literature

The formalisms found in literature were created based on slightly different systems and under different experimental conditions to the one studied in the current work, so their application to the current experimental results is likely to cause deviation. However, all involved the use of Sb_2O_3 as

catalyst in oligomerisation/polymerisation reactions, so it was desired to see their applicability in the current system.

4.3.1 Yamada formalism

In this formalism, \mathcal{FM} was considered as equal to $[Sb]$, the resulting expression for k is shown in Equation (5), where the parameters to be fitted are highlighted in bold [13], [14]. This formalism does not consider the catalytic inhibition of Sb_2O_3 by EG.

$$k(T) = \left\{ \mathbf{k}_{ref}^{th} + \mathbf{k}_{ref}^{cat} \times [Sb] \right\} \times \exp\left(-\frac{E_a}{R} \left[\frac{1}{T} - \frac{1}{T_{ref}} \right]\right) \quad (5)$$

The tuned values of each of these parameters, with the respective t-value are shown in Table 4.

Table 4: Tuned parameters in the Yamada formalism.

	Value	t-value	Final values
\mathbf{k}_{ref}^{th}	Val ₁	16.3	-
\mathbf{k}_{ref}^{cat}	Val ₂	47.9	-
E_a	96.2	8.17	96±6 kJ/mol

Figure 8 and Figure 9 show how the Yamada formalism fit two different sets of experimental results. Given that this formalism does not consider that EG inhibits the catalytic effect of Sb_2O_3 , it is interesting to observe its fitting at low and high values of $[Sb]$.

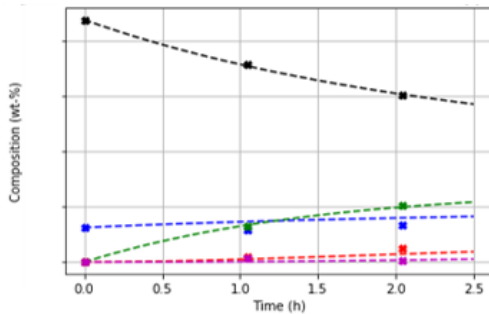


Figure 8: Condition 1: Low $[Sb]$; $T=180^\circ C$; $R^2=0.99$.

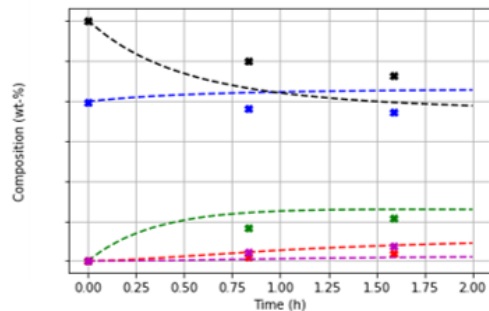


Figure 9: Condition 2: High $[Sb]$; $T=180^\circ C$; $R^2=0.45$.

The Yamada formalism showed a good fitting to the experimental results ($R^2 > 0.95$) when EG_0 was below ca. 25 wt-%, but a much inferior response when EG_0 was superior that value. This is because this formalism does not consider the inhibitory effect of EG, which means that it is only applicable when this effect is negligible, *i.e.*, when the amount of EG is low.

Figure 10 shows the BHET residuals for the Yamada formalism as a function of EG_0 . It is clear that the residuals become greater as the value of EG_0 increases.

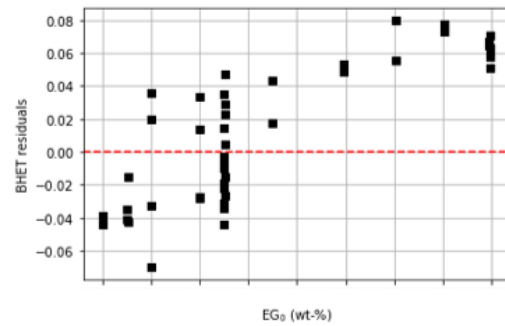


Figure 10: BHET residuals VS EG_0 for Yamada formalism.

4.3.2 Hovenkamp formalism

Unlike the previous, this formalism does take into account the inhibitory effect of EG on the catalytic activity of Sb_2O_3 . This modification is expressed by the addition of the parameter k_{inh} , and by adding a denominator to \mathcal{FM} , as shown in Equation (6) [10].

$$k(T) = \left\{ \mathbf{k}_{ref}^{th} + \mathbf{k}_{ref}^{cat} \times \frac{[Sb]}{1 + \mathbf{k}_{inh} \times [EG]} \right\} \times \exp\left(-\frac{E_a}{R} \left[\frac{1}{T} - \frac{1}{T_{ref}} \right]\right) \quad (6)$$

Only the value of k_{inh} was fitted for the Hovenkamp formalism, while the values of k_{ref}^{th} , k_{ref}^{cat} and E_a used were the same as the ones from the Yamada formalism.

Given that this formalism considers the inhibitory effect of EG, it is most interesting to see how well it fits to the experiments performed at higher EG_0 , which is the range of values at which inhibition is significant. However, it is also necessary to see if the addition of k_{inh} into the model affects its applicability to the experiments with lower EG_0 . Figure 11 and Figure 12 show two examples.

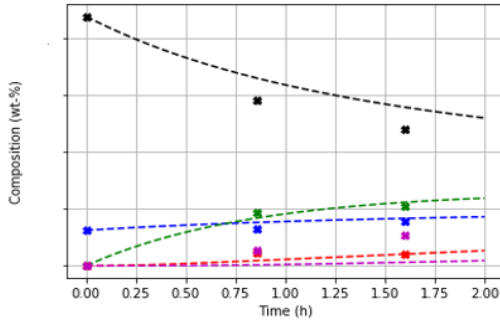


Figure 11: Condition 3: Low [Sb]; T=190°C; R²=0.92 (Yamada: R²=0.97).

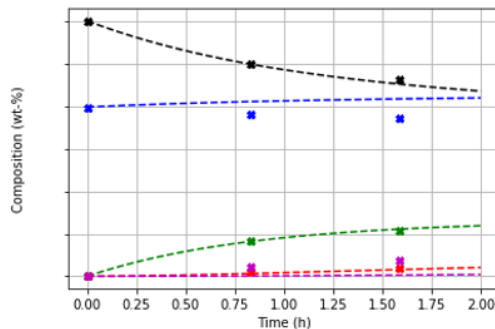


Figure 12: Condition 4: High [Sb]; T=180°C; R²=0.99 (Yamada, R²=0.45).

This formalism presents a much superior behaviour to the Yamada formalism for EG₀ above and equal to ca. 25 wt-%, *i.e.*, when the inhibitory effect is not negligible due to the high amount of EG present in the system. This superior behaviour is reflected in the higher values of R² for experiments in that range. However, this formalism presents, on average, an inferior fitting to the experimental results for the sets of experiments in which EG₀ is below ca. 25 wt-%.

Figure 13, which shows the BHET residuals for the Hovenkamp formalism as a function of EG₀. It is possible to see that, compared to the Yamada formalism, the Hovenkamp formalism shows much smaller residuals for higher values of EG₀, while slightly bigger for lower values of EG₀.

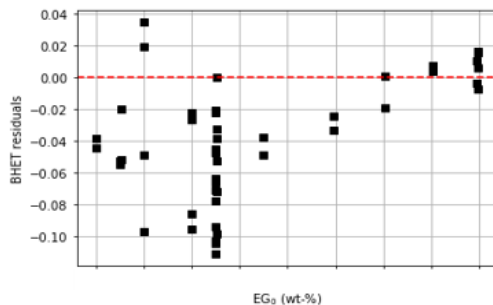


Figure 13: BHET residuals VS EG₀ for Hovenkamp formalism.

4.4 Proposed formalism

By defining three additional parameters, α , β and γ , which were added based on the observed behaviour of the rate of reaction with [Sb] for constant EG₀, Equation (7) was obtained.

$$k(T) = \left\{ k_{\text{ref}}^{\text{th}} + k_{\text{ref}}^{\text{cat}} \times \frac{\alpha + \beta \times [\text{Sb}]}{1 + (k_{\text{inh}} \times [\text{EG}])^\gamma} \right\} \times \exp\left(-\frac{E_a}{R} \left[\frac{1}{T} - \frac{1}{T_{\text{ref}}} \right]\right) \quad (7)$$

The values of $k_{\text{ref}}^{\text{th}}$, $k_{\text{ref}}^{\text{cat}}$, E_a and k_{inh} used were the same as the ones used in the previous formalism. Only α , β and γ were tuned. Figure 14 and Figure 15 depict how this formalism fits to two sets of experimental results, with different initial compositions.

It is possible to see that the values of R² for the proposed formalism were above 0.99 and either higher or equal to those of the formalisms from literature. This means that, for nearly all sets of experimental results, the proposed formalism has an equal or better response than those of the formalisms from literature and that the proposed formalism is able to accurately predict the experimental results for all experimental conditions.

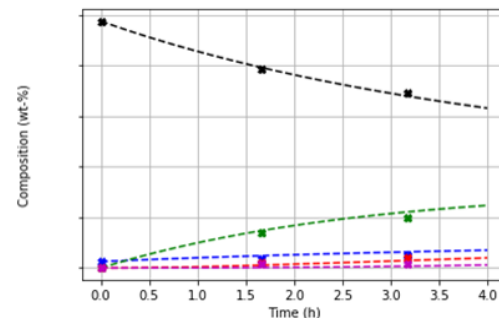


Figure 14: Condition 5: Low [Sb]; T=180°C; R²=0.99 (Yamada: R²=0.96, Hovenkamp: R²= 0.92).

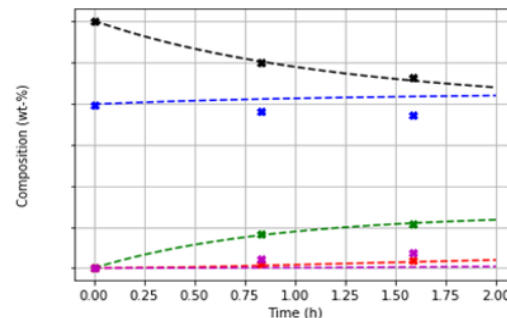


Figure 15: Condition 6: High [Sb]; T=180°C; R²=0.99 (Yamada: R²=0.45, Hovenkamp: R²= 0.99).

Figure 16 shows the BHET residuals for the proposed formalism as a function of EG₀. A similar

trend to Figure 13 is observed, but the residuals are generally smaller compared to the Hovenkamp formalism, especially for low EG_0 .

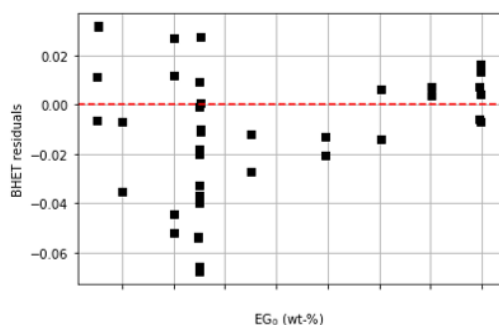


Figure 16: BHET residuals VS EG_0 for the proposed formalism.

5 Conclusions and work perspectives

5.1 Conclusions

Results show that the rate of reaction varied directly proportional to $[Sb]$ and the temperature, as it would be expected from catalysed kinetics. However, the effect of $BHET_0:EG_0$ ratio was not clear, because it required the comparison between reactions with different initial compositions, which greatly also affect the rate of reaction. The effect of the precursor of Sb_2O_3 on the rate of reaction was not clear either, probably due to the uncertainty in the measurement of the mass of Sb_2O_3 powder and the possible limit of solubility of Sb_2O_3 in the reaction medium.

Due to the unclear effect of $BHET_0:EG_0$ on the catalytic activity it was difficult to ascertain whether or not EG presents an inhibitory effect and to which extent. Thus, it was necessary to proceed to the modelling work.

As mentioned previously, the formalisms found in literature were proposed based on different systems and experimental conditions to the one studied in the current work. However, their applicability to the current system was observed.

By applying the tuned formalisms to the reactor model, it was possible to see clear trends. The Yamada formalism normally showed a good fitting to the experimental results ($R^2 > 0.95$) when EG_0 was below ca. 25 wt-%, while the Hovenkamp formalism normally showed a much superior fitting than Yamada to the experimental results when EG_0 was above and equal to ca. 25 wt-%. This is because the Hovenkamp formalism considers that EG inhibits the catalytic activity of Sb_2O_3 , while the Yamada formalism does not.

However, the Hovenkamp formalism showed a slightly inferior fitting than Yamada for EG_0 below ca. 25 wt-%. This is because k_{ref}^{th} , k_{ref}^{cat} and E_a tuned for the Yamada formalism were used as such in the Hovankamp formalism, and not refitted. Additionally, k_{inh} was tuned using different experimental results than k_{ref}^{th} and k_{ref}^{cat} , which may have caused the Hovenkamp formalism to have a worse prediction for low values of EG_0 .

The formalism proposed in the current work also considers that EG inhibits the catalytic activity of Sb_2O_3 , but it proposes a more complex correlation between k and $[Sb]$ than both formalisms from literature. It allowed for a good prediction of the experimental results for all ranges of $BHET:EG$ and $[Sb]$ studied in the current work, allowing for a wider range of applicability than that of both formalisms from literature. The values of R^2 obtained using the proposed formalism are usually superior to those of both formalisms from literature for a given set of experimental results.

5.2 Future perspectives

By carrying out the reaction inside autoclaves instead of glass reactors, a kinetic study of the same kinetic system, but on a different range of temperatures could be performed. In industry and in most articles found in literature, the polymerisation of PET was carried out at higher temperatures ($>200^\circ C$). The applicability of the tuned formalisms at these temperatures, as well as different ranges of $BHET_0:EG_0$ and $[Sb]$ could also be studied.

The use of different solvents, such as DEG, instead of EG, could also be investigated, as their effect on the catalytic activity of Sb_2O_3 is likely to be different. The use of different catalysts, such as $Sb(Ac)_3$, is also likely to affect the rate of reaction, as they form different active species in solution and cause the reaction to proceed through a different mechanism.

6 Bibliography

- [1] S. Mandal and A. Dey, "PET Chemistry," in *Recycling of Polyethylene Terephthalate Bottles*, 2018, pp. 1–22.
- [2] I. Tiseo, "Production of polyethylene terephthalate bottles worldwide from 2004 to 2021," 2021. <https://www.statista.com/statistics/723191/production-of-polyethylene-terephthalate-bottles-worldwide/> (accessed May 09, 2022).

- [3] Damayanti and H.-S. Wu, "Strategic Possibility Routes of Recycled PET," *Polymers (Basel)*, vol. 13, no. 9, 2021, doi: <https://doi.org/10.3390/polym13091475>.
- [4] H. W. Goh, A. Salmiaton, N. Abdullah, and A. Idris, "Time, Temperature and Amount of Distilled Water Effects on the Purity and Yield of Bis(2-hydroxyethyl) Terephthalate Purification System," *Bull. Chem. React. Eng. Catal.*, vol. 10, no. 2, pp. 143–154, 2015, doi: <https://doi.org/10.9767/bcrec.10.2.7195.143-154>.
- [5] IFPEN, "Contribution of Chemistry to Plastics Recycling." <https://www.ifpenergiesnouvelles.com/innovation-and-industry/our-expertise/climate-environment-and-circular-economy/plastics-recycling/our-solutions> (accessed Apr. 18, 2022).
- [6] A. Sheel and D. Pant, *Chemical Depolymerization of PET Bottles via Glycolysis*. Elsevier Inc., 2019.
- [7] S. H. Park and S. H. Kim, "Poly (ethylene terephthalate) recycling for high value added textiles," *Fash. Text.*, vol. 1, no. 1, pp. 1–17, 2014, doi: 10.1186/s40691-014-0001-x.
- [8] F. A. El-Toufaily, G. Feix, and K. H. Reichert, "Mechanistic investigations of antimony-catalyzed polycondensation in the synthesis of poly(ethylene terephthalate)," *J. Polym. Sci. Part A Polym. Chem.*, vol. 44, no. 3, pp. 1049–1059, 2006, doi: 10.1002/pola.21200.
- [9] S. B. Maerov, "Influence of Antimony Catalysts With Hydroxyethoxy Ligands on Polyester Polymerization.," *J. Polym. Sci. A1.*, vol. 17, no. 12, pp. 4033–4040, 1979, doi: 10.1002/pol.1979.170171223.
- [10] "Chapter 3: Reaction Kinetics," 2004.
- [11] Shodex™, "Lesson 6: Detectors for HPLC." <https://www.shodex.com/en/kouza/f.html#!> (accessed Sep. 07, 2022).
- [12] R. Rulken and C. Koning, "Polycondensation," in *Polymer Science: A Comprehensive Reference*, Elsevier, Ed. 2012, pp. 431–467.
- [13] T. Yamada, "Mathematical Model for a Semicontinuous Esterification Process with Recycle Between Terephthalic Acid and Ethylene Glycol," *J. Appl. Polym. Sci.*, vol. 45, no. 5, pp. 731–744, 1992.
- [14] B. Duh, "Effect of antimony catalyst on solid-state polycondensation of poly(ethylene terephthalate)," *Polymer (Guildf)*, vol. 43, no. 11, pp. 3147–3154, 2002, doi: 10.1016/S0032-3861(02)00138-6.